

Vanadyl C and N-capped tris(phenolate) complexes: influence of pro-catalyst geometry on catalytic activity†

Carl Redshaw,^{*a} Michael A. Rowan,^a Damien M. Homden,^a Sophie H. Dale,^b Mark R. J. Elsegood,^b Shigekazu Matsui^c and Sadahiko Matsuura^c

Received (in Cambridge, UK) 16th May 2006, Accepted 6th June 2006

First published as an Advance Article on the web 29th June 2006

DOI: 10.1039/b606897a

Vanadyl complexes of C or N-capped tripodal ligands, possessing distorted tetrahedral geometry at vanadium, serve as extremely active, thermally robust pro-catalysts for ethylene homo- and ethylene/propylene copolymerisation, whereas pseudo-octahedral pro-catalysts produce far lower activities.

In contrast to group 4 metals, highly active α -olefin polymerisation catalysts of group 5 are scarce,¹ this despite the commercial use of the [V(acac)₃] system in the production of ethylene-propylene-diene elastomers.² These poorer activities are associated with catalyst deactivation, typically *via* reduction to the divalent state, a problem more prevalent under the elevated temperatures associated with commercial conditions. Fujita *et al.* have prepared the first examples of highly active (up to 65 000 g mmol⁻¹ h⁻¹ bar⁻¹), thermally robust (75 °C) vanadium-based olefin polymerisation catalysts.³ Gibson *et al.*, Nomura *et al.* and ourselves have utilized dialkylaluminium chlorides in the presence of the reactivator ethyl trichloroacetate (ETA) to generate highly active vanadium-based systems incorporating mono- or bidentate ancillary ligands.⁴ However, the use of macrocyclic ligands, most notably calixarenes, has met with limited success in this type of catalysis.⁵ Herein, we turn our attention to tripodal ligands, specifically tris(3,5-di-*tert*-butyl-2-hydroxyphenyl/benzyl)methane (C-capped) and tris(2-hydroxyphenyl)amine (N-capped). These ligands, in particular the C-capped benzyl analogue, have been utilised in a variety of polymerisation studies, including the copolymerisation of cyclohexene oxide/carbon dioxide^{6a} and lactide polymerisation.^{6b-d} Kawaguchi and co-workers have also recently reported a number of *syn*- and *anti*-complexes of the C-capped ligand system and noted interesting structural features.⁷

The vanadyl pro-catalysts (Fig. 1) are readily accessible as red (1, 6), pale green (2) or blue (3, 4, 5) crystalline solids in good yield (75–85% (1, 3, 4 and 6), 65% (5) and 44% (2)) *via* the reaction of the parent tripodal ligand with the alkoxide [VO(OPr^{*t*})₃].‡ The C-capped oxo pro-catalyst, 1, is dimeric (Fig. 2, left) and sits on an inversion centre with half a molecule in the asymmetric unit. It is best described as a 16-membered metalocycle comprising two bridging vanadium centres (η^1 to one C-capped ligand, η^2 to the

other), four oxygens and ten carbons. The two 8-membered rings containing O(2) and O(2A) are folded such that the phenyl groups are orientated approximately axial with respect to the macrocycle plane and point in the same direction as each distorted tetrahedral vanadyl grouping.

In an attempt to form a monomeric complex, a 2,6-di(isopropyl)phenylimino arm was appended to the parent ligand using the method of Scott *et al.*⁸ Treatment of this new imine ligand, LH₃, with [VO(OPr^{*t*})₃] in refluxing toluene led to reduction and formation of the bis-chelate complex [V(LH₂)₂], 2, in *ca.* 45% yield. Complex 2 has approximate C₂ symmetry (Fig. 1, centre), and the chelate ligands bind in their salicylaldimine (phenoxymimine) form in a *trans* fashion to afford the base of the essentially square-based pyramidal vanadyl centre. As well as H-bonding involving O(1)/O(4), there are also intramolecular O–H... π interactions present (H(3)–(centroid of C(25)–C(30)) = 2.759 Å, angle at H(3) = 159.7°; H(6)–(centroid of C(77)–C(82)) = 2.896 Å, angle at H(6) = 165.1°).

Encouraged by the catalytic behaviour of 1 *vide infra*, we extended our studies to the analogous N-centred ligand system. The N-capped oxo complex 3 (Fig. 2, right), structurally characterised using synchrotron radiation,⁹ possesses a distorted octahedral vanadyl centre, the coordination sphere of which is completed by a solvent molecule (MeCN). The vanadium lies 0.321 Å above the plane defined by the three oxygen atoms of the tripod ligand and the nitrogen of MeCN.

Catalytic results for 3 were less impressive, and in order to determine whether the presence of the metal-bound MeCN was detrimental, this reaction was carried out solely in toluene. X-Ray studies, again using synchrotron radiation,⁹ reveal that a *n*-propanol molecule, arising from the loss of alcohol during the

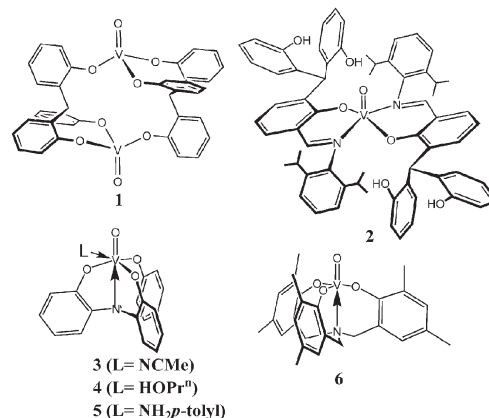


Fig. 1 The vanadyl pro-catalysts. *tert*-Butyl groups omitted for clarity.

^aWolfson Materials and Catalysis Centre, School of Chemical Sciences and Pharmacy, University of East Anglia, Norwich, Norfolk, UK NR4 7TJ. E-mail: carl.redshaw@uea.ac.uk; Tel: +44 (0)1603 593137

^bChemistry Department, Loughborough University, Loughborough, Leicestershire, UK LE11 3TU. E-mail: M.R.J.Elsegood@lboro.ac.uk
^cR & D Center, Mitsui Chemicals, Inc., 580-32 Nagaura, Sodegaura, Chiba 299-0265, Japan

† Electronic supplementary information (ESI) available: Crystal summary data for 1–5 and LH₃. See DOI: 10.1039/b606897a

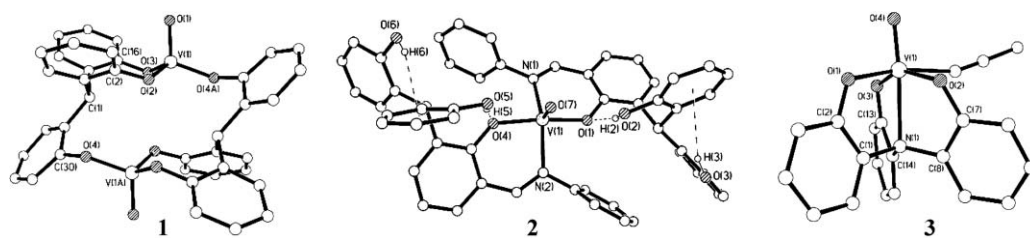


Fig. 2 The molecular structures of **1**, **2** and **3** respectively. Selected bond lengths (Å) and angles (°). **1**: V(1)–O(1) 1.585(2), V(1)–O(2) 1.7828(19), V(1)–O(3) 1.7774(19), V(1)–O(4A) 1.7877(18), V(1)–O(2)–C(2) 131.29(16), V(1)–O(3)–C(16) 128.92(17); atoms labelled **A** are at (1 – *x*, 1 – *y*, 1 – *z*). **2**: V(1)–O(1) 1.936(4), V(1)–O(7) 1.582(4), V(1)–N(1) 2.102(5), O(7)–V(1)–O(4) 100.4(2), O(4)–V(1)–O(1) 158.91(18), N(1)–V(1)–O(1) 86.67(19). **3**: V(1)–O(1) 1.8658(13), V(1)–O(2) 1.8632(13), V(1)–O(3) 1.8498(13), V(1)–O(4) 1.5889(13), V(1)–N(1) 2.3765(14), V(1)–N(2) 2.1657(16), O(1)–V(1)–O(2) 94.93(6), O(1)–V(1)–N(1) 79.53. *tert*-Butyl and isopropyl groups omitted for clarity.

reaction, binds to the pseudo-octahedral vanadium centre and occupies the position previously associated with the MeCN. Furthermore, carrying out the reaction in the presence of NH₂-*para*-tolyl leads to similar complex **5**, in which the aniline binds at the position occupied by the MeCN in **3**. Introduction of an extra methylene group into each arm of the N-capped ligand allows access to the 5-coordinate vanadyl complex **6**, the structure of which has recently been reported.¹⁰

In catalytic screening (Table 1) using dimethylaluminium chloride (DMAC) and ETA, **1** and **6** demonstrated significantly greater activity (up to 123 000 g mmol⁻¹ h⁻¹ bar⁻¹) relative to **2–5**. If preserved, the bis(chelate) nature of **2** may be hampering its performance, and the presence of the ‘free’ phenolic groups on each phenoxyimine provide alternative reactive sites for the co-catalyst. However, the lower activity of **3** (results for **4** and **5** were similar—*ca.* 1000 g mmol⁻¹ h⁻¹ bar⁻¹ at 25 °C) relative to **6** does not seem to be due to the presence of MeCN, rather that the sixth position is occupied by ‘a ligand’, be it MeCN, *n*-PrOH or NH₂-*para*-tolyl.

Occupation of this site can be prevented by increasing the ‘bite’ of the N-capping ligand through introduction of a methylene linker into each arm (**6**); the result is a large increase in the observed catalytic activity. This also leads to an increase in the V(1)–N(1) ‘cap’ distance (*i.e.*, 2.4697(4) Å for **6**: cf. 2.3765(14) Å in **3**, 2.377(3) Å in **4** and 2.390(4) Å (*av.*) in **5**) and thus the geometry at vanadium in **6** can be considered to more closely approach that of **1**.

Notably, there is a pronounced increase in activity with increasing temperature for catalytic systems utilising **1**, **2** and **6**, leading to some of the highest observed activities to date for vanadium-based systems. The effect of temperature is much less pronounced for **3–5**; in all cases there is a concomitant decrease in polymer molecular weight. Ultra-high molecular

weight polyethylene is obtained in all cases at 25 °C; the melting points (133.0–134.5 °C) obtained by DSC are typical of linear polyethylene. The nature (and amount) of the co-catalyst used is crucial. For example, methylaluminoxane (MAO) gives far inferior activities. Activities (and lifetimes) are substantially reduced in the absence of ETA.

For ethylene/propylene copolymerisation (Table 2), the activities of **1–3** and **6** follow the same trend as for ethylene, with high activities observed for **1** (6 000 g mmol⁻¹ h⁻¹ bar⁻¹) and **6** (12 000 g mmol⁻¹ h⁻¹ bar⁻¹), and with 14.6 and 15.0 mol% propylene incorporation, respectively, but a much lower activity value for **2** (1 300 g mmol⁻¹ h⁻¹ bar⁻¹) and **3** (60 g mmol⁻¹ h⁻¹ bar⁻¹).

The exact role played by DMAC in obtaining such phenomenal activities is far from clear. However, similarities between activities, molecular weights and polydispersity (PDI) values for a number of these systems suggest that related active species are formed in certain cases, *e.g.* **1** and **6** or **3–5**. Furthermore, the coordination geometry at vanadium in **1** closely approaches that observed in the highly active vanadyl triphenolate complexes [V(O)L]₂ (L = OArCH₂Ar'(O)CH₂ArO, Ar = 4,6-di-*tert*-butylphenyl or 4-methyl-6-*tert*-butylphenyl, Ar' = 4-methylphenyl).^{4b}

EPR spectra, recorded upon addition of excess DMAC, are complex. For **1**, reducing the amount of DMAC to <10 equiv. affords spectra typical of two interacting vanadium species, *viz* two features at *ca.* *g* = 2 and 4, both with greater than 10 lines. The appearance of a transition arising from the triplet state in the half-field region provides strong support for the existence of dimers. Quantitative studies of **1** against a standard of known concentration [VO(*acac*)₂] suggest that there is an appreciable amount of V(IV) formed upon addition of excess DMAC. For 10 equiv. of DMAC, when ETA is absent, the concentration of V(IV) remains constant at *ca.* 33% over 1 h. In the presence of ETA, the initial (1 min) concentration of V(IV) is *ca.* 60%, which falls to 33% after

Table 1 Ethylene polymerisation results^a

| Pro-catalyst | <i>T</i> /°C | Yield/g | Activity ^b | <i>M</i> _w ^c | <i>M</i> _n ^d | PDI ^e |
|--------------|--------------|---------|-----------------------|------------------------------------|------------------------------------|------------------|
| 1 | 25 | 1.17 | 22 300 | 6 860 000 | 1 760 000 | 3.9 |
| 1 | 80 | 6.20 | 122 900 | 387 000 | 175 000 | 2.2 |
| 2 | 25 | 0.29 | 5 900 | — | — | — |
| 2 | 80 | 1.24 | 24 900 | — | — | — |
| 3 | 25 | 0.08 | 1 500 | 8 670 000 | 3 460 000 | 2.5 |
| 3 | 80 | 0.12 | 2 300 | 556 000 | 273 000 | 2.0 |
| 6 | 25 | 1.40 | 28 100 | 5 180 000 | 1 590 000 | 3.3 |
| 6 | 80 | 4.18 | 96 500 | 481 000 | 234 000 | 2.0 |

^a 250 ml toluene, 1 bar C₂H₄, 0.2 μmol pro-catalyst, 0.5 mmol DMAC, 0.5 mmol ETA for 15 min. ^b Measured in g mmol⁻¹ h⁻¹ bar⁻¹. ^c Weight average molecular weight. ^d Number average molecular weight. ^e Polydispersity index.

Table 2 Ethylene/propylene copolymerisation results at 25 °C^a

| Pro-catalyst | Yield/g | Activity ^b | <i>M</i> _w | <i>M</i> _n | PDI | C ₃ incorporation (mol%) ^c |
|--------------|---------|-----------------------|-----------------------|-----------------------|-----|--|
| 1 | 0.29 | 6 000 | 2 000 000 | 1 000 000 | 2.0 | 14.6 |
| 2 | 0.07 | 1 300 | — | — | — | — |
| 3 | 0.003 | 600 | — | — | — | — |
| 6 | 0.62 | 12 400 | 3 010 000 | 1 310 000 | 2.3 | 15.0 |

^a 250 ml toluene, 1 bar 50 : 50 C₂H₄/C₃H₆, 0.2 μmol pro-catalyst, 0.5 mmol DMAC, 0.5 mmol ETA for 15 min. ^b Measured in g mmol⁻¹ h⁻¹ bar⁻¹. ^c Percentage incorporation of propyl unit into polymer.

1 h. Results using 500 equiv. of DMAC in the presence of ETA are similar, though the high levels of DMAC are detrimental to the quality of the spectra. Given the observed beneficial results played by ETA on the activity of this system, these EPR results suggest the role played by ETA is to reintroduce V(III) into the cycle, a role which is more pronounced at elevated temperatures. Previous EPR studies on vanadium-based soluble Ziegler-type catalysts suggest that these systems are complex, forming multiple species, e.g., the $[\text{Cp}_2\text{VCl}_2]/\text{EtAlCl}_2$ system formed at least three EPR active species, one of which was identified as $[\text{Cp}_2\text{VCl}(\mu\text{-Cl})_2\text{AlCl}_2]^{11a}$ later, the hydride $[\text{Cp}_2\text{VH}(\mu\text{-Cl})_2\text{AlCl}_2]$ was also proposed.^{11b}

At this stage the exact geometry of the active species is not known, nor is how it relates to the pro-catalyst structure, and so we tentatively propose a pro-catalyst structure–activity relationship.

In summary, we have demonstrated that highly active, thermally robust, vanadium-based catalysts are accessible using a C or N-capped tripodal system as an ancillary ligand. The differing geometrical constraints of the C and N-capped ligands are highlighted by crystal structure analyses of these vanadyl derivatives. The catalytic results of **1–6** suggest a trend towards higher activity if octahedral coordination can be avoided in the pro-catalyst.

The EPSRC (INTERACT Japan) is thanked for financial support, and for the award of beam time at the SRS, Daresbury Laboratory stations 9.8 and 16.2 SMX. We thank the EPSRC Mass Spectrometry Service Centre, Swansea and the X-Ray Crystallography Service, Southampton for data collection for **2**.

Notes and references

† Selected spectroscopic data. For **1**: $\text{C}_{86}\text{H}_{122}\text{O}_8\text{V}_2$ calc. % (found %) C, 74.54 (74.16); H, 8.87 (9.03). ^1H NMR (CDCl_3 , 400 MHz): δ 7.21 (s, 2 H, Ar–H), 7.29 (s, 2 H, Ar–H), 7.22 (s, 2 H, Ar–H), 7.21 (s, 2 H, Ar–H), 7.11 (s, 2 H, Ar–H), 4.79 (s, 2 H, Ar₃CH), 1.41 (s, 18 H, ArCH₃), 1.28 (s, 18 H, ArCH₃), 1.22 (s, 36 H, C(CH₃)₃) and 1.20 (s, 36 H, C(CH₃)₃). ^{51}V NMR (CDCl_3 , 105.1 MHz): δ –298.4 (ω_{vs} = 382 Hz), (C_6D_6): δ –307.8 (ω_{vs} = 257 Hz). MS (EI): 692.4 ($\frac{1}{2}\text{M}^+$), 693.4 ($\frac{1}{2}\text{M} + \text{H}$)⁺. M.p. = 259–261 °C.

For **2**: $\text{C}_{104}\text{H}_{144}\text{N}_5\text{O}_7\text{V}$ -0.5 CH_2Cl_2 calc. % (found %) C, 77.15 (76.90); H, 9.00 (9.04); N, 1.71 (1.66). ^1H NMR (CDCl_3 , 400 MHz): δ 8.30 (s, 1 H, CH=N), 6.5–7.4 (bm, 9 H, Ar–H), 6.06 (s, 1 H, Ar₃CH), 5.41 (s, 2 H, OH), 4.91 (bs, 2 H, OH), 2.83 (bm, 2 H, (CH₃)₂CH) and 0.2–2.1 (5 bm, 7 H, (CH₃)₂CH and C(CH₃)₃). ^{51}V (CDCl_3 , 105.1 MHz): δ –72.44 (ω_{vs} = 370 Hz). MS (EI): 1585 (M – 2H)⁺. M.p. > 250 °C. Magnetic moment $\mu = 1.76\mu_{\text{B}}$. EPR (toluene, 298 K): $g_{\text{iso}} = 1.99$, $A_{\text{iso}} = 94$ G, (toluene, 10 K): $g_{\perp} = 1.98$, $A_{\perp} = 67$ G, $g_{\parallel} = 1.95$, $A_{\parallel} = 185$ G.

For **3**: $\text{C}_{18}\text{H}_{12}\text{N}_1\text{O}_4\text{V}$ -0.75MeCN calc. % (found %) C, 60.36 (59.92); H, 3.69 (3.67); N, 6.31 (6.24). ^1H NMR (400 MHz, CDCl_3 , 298 K): δ 7.79 (d, 3 H, Ar–H, $^3J_{\text{HH}} = 6.6$ Hz), 7.29 (t, 3 H, Ar–H, $^3J_{\text{HH}} = 7.3$ Hz), 7.01 (t, 3 H, Ar–H, $^3J_{\text{HH}} = 7.3$ Hz), 6.65 (d, 3 H, Ar–H, $^3J_{\text{HH}} = 6.6$ Hz) and 2.06 (s, 3 H, CH₃ of MeCN). ^{51}V (CDCl_3 , 105.1 MHz): δ –295. MS (EI): 358 (M – MeCN)⁺, 399 (M + H)⁺.

For **4**: $\text{C}_{21}\text{H}_{20}\text{NO}_4\text{V}$ -0.33toluene calc. % (found %) C, 62.54 (62.75); H, 5.11 (5.23); N, 3.12 (2.85). ^1H NMR (C_6D_6 , 400 MHz): δ 7.21 (d, 3 H, Ar–H, $^3J_{\text{HH}} = 8.3$ Hz), 6.69 (t, 3 H, Ar–H, $^3J_{\text{HH}} = 7.5$ Hz), 6.71 (d, 2 H, tolyl–H, $^3J_{\text{HH}} = 7.0$ Hz), 6.32 (d, 3 H, Ar–H, $^3J_{\text{HH}} = 8.2$ Hz), 3.23 (t, 2 H, OCH₂CH₂CH₃, $^3J_{\text{HH}} = 7.4$ Hz), 2.10 (s, 1 H, OH), 1.21 (m, 2 H, OCH₂CH₂CH₃, $^3J_{\text{HH}} = 7.4$ Hz) and 0.65 (t, 3 H, OCH₂CH₂CH₃, $^3J_{\text{HH}} = 7.4$ Hz). ^{51}V (CDCl_3 , 105.1 MHz): δ –305.1 (ω_{vs} = 130 Hz). MS (EI): 358 (M – HOPrⁿ). M.p. = 239–240 °C.

For **5**: $\text{C}_{25}\text{H}_{21}\text{N}_2\text{O}_4\text{V}$ -0.66MeCN calc. % (found %) C, 64.32 (64.22); H, 4.72 (4.75); N, 7.59 (7.62). ^1H (C_6D_6 , 400 MHz): δ 7.27 (d, 3 H, Ar–H, $^3J_{\text{HH}} = 8.3$ Hz), 6.71 (t, 3 H, Ar–H, $^3J_{\text{HH}} = 7.5$ Hz), 6.71 (d, 2 H, tolyl–H, $^3J_{\text{HH}} = 8.2$ Hz), 6.51 (t, 3 H, Ar–H, $^3J_{\text{HH}} = 7.5$ Hz), 6.39 (d, 3 H, Ar–H, $^3J_{\text{HH}} = 8.3$ Hz), 6.25 (d, 2 H, tolyl–H, $^3J_{\text{HH}} = 8.2$ Hz), 3.23 (bs, 2 H, NH₂), 2.03 (s, 3 H, tolyl–CH₃) and 0.57 (s, 3 H, MeCN). ^{51}V (CDCl_3 , 105.1 MHz): δ –334.1 (ω_{vs} = 160 Hz). MS (ES): 465 (M)⁺. M.p. = 198–200 °C.

Crystal data for **1**: $\text{C}_{86}\text{H}_{122}\text{O}_8\text{V}_2$, $M = 1385.72$, triclinic, space group $P\bar{1}$, $a = 12.1275(8)$, $b = 13.7705(10)$, $c = 13.8307(10)$ Å, $U = 2015.2(2)$ Å³, $\alpha = 104.984(2)$, $\beta = 104.898(2)$, $\gamma = 105.394(2)^\circ$, $T = 150(2)$ K, $Z = 1$,

$\mu(\text{Mo-K}\alpha) = 0.284$ mm^{–1}, $\lambda = 0.71073$ Å, 17569 reflections measured, 8979 unique ($R_{\text{int}} = 0.0343$) which were used in all calculations. The final $wR^2 = 0.1467$ (all data) and $R1 = 0.0567$ (for 5954 data with $F^2 > 2\sigma(F^2)$). CCDC 607716.

Crystal data for **2**: $\text{C}_{104}\text{H}_{144}\text{N}_5\text{O}_7\text{V}$, $M = 1585.15$, monoclinic, space group $P2_1/c$, $a = 15.4639(8)$, $b = 30.6728(17)$, $c = 21.4928(9)$ Å, $U = 9743.5(8)$ Å³, $\beta = 107.107(3)^\circ$, $T = 120(2)$ K, $Z = 4$, $\mu(\text{Mo-K}\alpha) = 0.154$ mm^{–1}, $\lambda = 0.71073$ Å, 64432 reflections measured, 12660 unique ($R_{\text{int}} = 0.2112$) which were used in all calculations. The final $wR^2 = 0.1859$ (all data) and $R1 = 0.1009$ (for 6643 data with $F^2 > 2\sigma(F^2)$). CCDC 607717.

Crystal data for **3**: $\text{C}_{20}\text{H}_{15}\text{N}_2\text{O}_4\text{V}$, $M = 398.28$, monoclinic, space group $P2_1/n$, $a = 9.6923(18)$, $b = 11.754(2)$, $c = 16.214(3)$ Å, $U = 1764.5(6)$ Å³, $\beta = 107.213(4)^\circ$, $T = 150(2)$ K, $Z = 4$, $\mu = 0.591$ mm^{–1}, $\lambda = 0.6892$ Å, 12369 reflections measured, 4942 unique ($R_{\text{int}} = 0.0466$) which were used in all calculations. The final $wR^2 = 0.1179$ (all data) and $R1 = 0.0432$ (for 4077 data with $F^2 > 2\sigma(F^2)$). CCDC 607718.

Crystal data for **4**: $\text{C}_{24.5}\text{H}_{24}\text{NO}_5\text{V}$, $M = 463.39$, monoclinic, space group $P2_1/c$, $a = 23.7193(13)$, $b = 9.6174(5)$, $c = 21.0836(12)$ Å, $U = 4321.7(4)$ Å³, $\beta = 116.030(2)^\circ$, $T = 120(2)$ K, $Z = 8$, $\mu = 0.496$ mm^{–1}, $\lambda = 0.6751$ Å, 25481 reflections measured, 7242 unique ($R_{\text{int}} = 0.0680$). The final $wR^2 = 0.1063$ (all data) and $R1 = 0.0439$ (for 4922 data with $F^2 > 2\sigma(F^2)$). CCDC 607719.

Crystal data for **5**: $\text{C}_{27}\text{H}_{24}\text{N}_3\text{O}_4\text{V}$, $M = 505.43$, monoclinic, space group $P2_1$, $a = 9.2526(7)$, $b = 25.7210(18)$, $c = 9.8995(7)$ Å, $U = 2355.9(3)$ Å³, $\beta = 90.085(2)^\circ$, $T = 120(2)$ K, $Z = 4$, $\mu = 0.461$ mm^{–1}, $\lambda = 0.6751$ Å, 17474 reflections measured, 8056 unique ($R_{\text{int}} = 0.0453$) which were used in all calculations. The final $wR^2 = 0.0966$ (all data) and $R1 = 0.0431$ (for 7594 data with $F^2 > 2\sigma(F^2)$). CCDC 607720.

Crystal data for ligand **LH3**: $\text{C}_{53}\text{H}_{73}\text{NO}_3$, $M = 760.11$, triclinic, space group $P\bar{1}$, $a = 14.452(2)$, $b = 14.819(2)$, $c = 14.999(2)$ Å, $U = 2467.8(7)$ Å³, $\alpha = 116.865(2)$, $\beta = 116.214(2)$, $\gamma = 91.421(3)^\circ$, $T = 150(2)$ K, $Z = 2$, $\mu(\text{Mo-K}\alpha) = 0.062$ mm^{–1}, $\lambda = 0.8464$ Å, 12956 reflections measured, 6318 unique ($R_{\text{int}} = 0.0577$) which were used in all calculations. The final $wR^2 = 0.2253$ (all data) and $R1 = 0.0776$ (for 4298 data with $F^2 > 2\sigma(F^2)$). CCDC 607721. For crystallographic data in CIF or other electronic format see DOI: 10.1039/b606897a

- (a) H. Hagen, J. Boersma and G. van Koten, *Chem. Soc. Rev.*, 2002, **31**, 357; (b) S. Gambarotta, *Coord. Chem. Rev.*, 2003, **237**, 229.
- W. Kaminsky and M. Arndt, in *Applied Homogeneous Catalysis with Organometallic Compounds*, ed. B. Cornils and W. A. Hermann, VCH, Weinheim, Germany, 1996, vol. 1, pp. 220.
- (a) Y. Nakayama, H. Bando, Y. Sonobe, Y. Suzuki and T. Fujita, *Chem. Lett.*, 2003, **32**, 766; (b) Y. Nakayama, H. Bando, Y. Sonobe and T. Fujita, *J. Mol. Catal. A: Chem.*, 2004, **213**, 141.
- (a) K. Nomura, A. Sagara and Y. Imanishi, *Macromolecules*, 2002, **35**, 1583; (b) C. Redshaw, L. Warford, S. H. Dale and M. R. J. Elsegood, *Chem. Commun.*, 2004, 1954; (c) A. K. Tomov, V. C. Gibson, D. Zaher, S. H. Dale and M. R. J. Elsegood, *Chem. Commun.*, 2004, 1956; (d) W. Wang and K. Nomura, *Macromolecules*, 2005, **38**, 5905.
- (a) O. V. Ozerov, N. P. Rath and F. T. Ladipo, *J. Organomet. Chem.*, 1999, **586**, 223; (b) Y. Chen, Y. Zhang, Z. Shen, R. Kou and L. Chen, *Eur. Polym. J.*, 2001, **37**, 1181; (c) V. C. Gibson, C. Redshaw and M. R. J. Elsegood, *J. Chem. Soc., Dalton Trans.*, 2001, 767; (d) G. S. Long, B. Snedeker, K. Bartosh, M. L. Werner and A. Sen, *Can. J. Chem.*, 2001, **79**, 1026; (e) C. Capacchione, P. Neri and A. Proto, *Inorg. Chem. Commun.*, 2003, **6**, 339.
- (a) M. B. Dinger and M. J. Scott, *Inorg. Chem.*, 2001, **40**, 1029; (b) Y. Kim and J. G. Verkade, *Organometallics*, 2002, **21**, 2395; (c) Y. Kim, P. N. Kapoor and J. G. Verkade, *Inorg. Chem.*, 2002, **41**, 4834; (d) Y. Kim, G. K. Jnaneshwara and J. G. Verkade, *Inorg. Chem.*, 2003, **42**, 1437.
- F. Akagi, T. Matsuo and H. Kawaguchi, *J. Am. Chem. Soc.*, 2005, **127**, 11936.
- A. Cottone, III, D. Morales, J. L. Lecuire and M. J. Scott, *Organometallics*, 2002, **21**, 418.
- (a) W. Clegg, M. R. J. Elsegood, S. J. Teat, C. Redshaw and V. C. Gibson, *J. Chem. Soc., Dalton Trans.*, 1998, 3037; (b) W. Clegg, *J. Chem. Soc., Dalton Trans.*, 2000, 3223.
- S. Groysman, I. Goldberg, Z. Goldschmidt and M. Kol, *Inorg. Chem.*, 2005, **44**, 5073.
- (a) A. G. Evans, J. C. Evans and E. H. Moon, *J. Chem. Soc., Dalton Trans.*, 1974, 2390; (b) A. G. Evans, J. C. Evans and J. Mortimer, *J. Am. Chem. Soc.*, 1979, **101**, 3204.